Cumhuriyet Sci. J., 44(1) (2023) 188-196
DOI: https://doi.org/10.17776/csj.1112531

Cumhuriyet Science Journal

| csj.cumhuriyet.edu.tr | Founded: 2002 ISSN: 2587-2680 e-ISSN: 2587-246X Publisher: Sivas Cumhuriyet University

Ibuprofen and Paracetamol when They Meet: Quantum Theory of Atoms in Molecules Perspective

Cemal Parlak [1,a], Özgür Alver [2,b], Özge Bağlayan [2,c,*], Onur Demirel [3,d]

[1] *Department of Physics, Ege University, Science Faculty, İzmir, 35100, Türkiye*
[2] *Department of Physics, Eskisehir Technical University, Science Faculty, Eskisehir, 26470, Türkiye*
[3] *Faculty of Mathematics and Physics, Department of Physics, Freiburg Albert-Ludwigs University, Germany*
**Corresponding author*

Research Article

History
Received: 05/05/2022
Accepted: 16/11/2022

ABSTRACT

Ibuprofen (IBP) and paracetamol (PCM) are widely used and prescribed two drugs for particularly their effects in reducing pain and fever. For enhanced pain relief, combinations of IBP and PCM are considered another option rather than taken each drug alone. In the scope of this work, the possible structural interaction edges, some important electronic properties and the binding energy evaluations of the IBP&PCM system were examined with density functional theory (DFT) and quantum theory of atoms in molecules (QTAIM). Further, all the configurations were subjected to biological activity evaluations. It was observed that hydrogen bonding interactions are possible for the examined drug couple and configuration 4 is the most stable form whereas C1 and C6 are better inhibitors. Therefore, possible advantages and disadvantages or possible side effects must be taken into account before combining these two important drug molecules.

Keywords: Ibuprofen, Paracetamol, DFT, Hydrogen bonding, QTAIM.

[a] *cemal.parlak@ege.edu.tr* *https://orcid.org/0000-0002-6115-6098*
[b] *ozguralver@eskisehir.edu.tr* *https://orcid.org/0000-0003-0647-4242*
[c] *obaglayan@eskisehir.edu.tr* *https://orcid.org/0000-0002-0753-0325*
[d] *onurdemirel2626@gmail.com* *https://orcid.org/0000-0001-9695-9141*

Introduction

Ibuprofen and paracetamol are widely prescribed two drugs all over the world. IBP is known as a nonsteroidal anti-inflammatory drug and is extensively prescribed for the treatment of pain and inflammation [1, 2]. IBP is bound and transported in blood plasma with the help of proteins and particularly through human serum albumin [3]. Although they have different action mechanisms, PCM is also used for its analgesic, antipyretic and anti-inflammatory activities [4, 5]. In various cases such as postoperative pain, dysmenorrhoea and musculoskeletal pain the combination of IBP and PCM appeared as an effective treatment method [6-10].

At the theoretical level, DFT provides useful information about the structural properties of different types of molecular systems [11-13]. QTAIM has been widely used to analyze the real space functions and nature of interactions in various molecular systems, and to classify and understand bonding interactions in terms of a quantum mechanical parameter as electron density at the bond critical points [12-15]. Moreover, natural bond orbital (NBO) analysis provides an efficient technique for the study of hydrogen bonding interactions. It also offers a convenient basis for investigating charge transfer or conjugative interactions in molecular systems [11, 12, 16, 17].

Taking the advantages of DFT method, it is possible to find out the most possible structural energy configurations and interaction sites of the examined molecular systems. In the framework of this work, the interaction mechanisms and type of the interaction between IBP and PCM were investigated. The way they interacted and the molecular structures they build are considered important parameters for their effective treatment procedure. The blood plasma is the combination of large numbers of molecules which appears as a major limitation of this work. However, the possibility of IBP and PCM interaction should not be underestimated.

Computational Methods

IBP and PCM were first optimized by imposing no geometrical restrictions. Vibrational frequency calculations were carried out as well to see that the structures converged to a certain minimum. If any imaginary frequencies were observed at the end of vibrational frequency calculations, optimization procedures were repeated by applying small geometrical changes to the parts of the molecules where the imaginary frequencies were observed. Initial geometry configurations are very important to reach the correct optimum geometrical configurations at the end of the calculations [18]. Therefore, taking into account the previously reported works, –OH, –C=O and –NH of IBP and

PCM were selected as possible interaction sites [19, 20]. Six possible configurations were built with GaussView visualization program [21]. After building the structures, they were optimized in the way as it was mentioned above. The resultant optimized structures are given in Figures 1-6.

The binding energy calculations (E_b) between IBP and PCM were calculated as follows [22]:

$$E_b = E_{IBP\&PCM} - (E_{IBP} + E_{PCM})$$

In the given equation, $E_{IBP\&PCM}$, E_{IBP} and E_{PCM} are the optimized energies of the related structures. In the resultant E_b values, the basis sets superposition errors (BSSE) were also taken into account and calculated with the counterpoise correction method [23, 24].

The strength and the nature of possible bonding interaction sites of IBP and PCM were examined based on the QTAIM evaluations [14, 15]. In order to carry out a quantitative investigation of charge distributions and further understanding of the nature of interactions, NBO analyses were also performed [16, 17].

For the molecular optimizations of the structures from C1 to C6, the B3LYP method and 6-31G(d) basis set which yield widely acceptable results were used [25, 26]. Multiwfn program was employed for the calculations of topological parameters [14]. Finally, all the optimization and vibrational frequency calculations were carried out with Gaussian program [27]. The physicochemical properties and druglikeness of IBP...PCM were predicted by using the SwissADME website (http://swissadme.ch) [28].

Results and Discussion

In this part, all the possible conformers undertaken in this work were examined briefly taking into account the binding energies and structural properties. This is followed by the discussion of structure & biological activity relation and electronic properties.

Conformer C1

The optimized structure and the interaction sites for IBP and PCM for C1 are given in Figure 1. NBO charges of +0.242 / -0.692 for –CH / –OH and +0.507 / -0.612 for –OH / -C=O make the interaction possible for the examined conformer C1. Here NBO charges belong to the atoms given in bold letters. E_b energies were found as -7.38 and -5.09 kcal/mol, respectively. It is seen that in the water media the strength of the interaction lowered compared to gas phase calculations.

Some important topological parameters of bond critical points (BCPs) in the examined IBP&PCM system are given in Table 1. In Figure 1, the molecular topography map of the system is given. In the given map, illustrated lines show bond paths. In C1, two possible intermolecular hydrogen bondings were proposed. The first one is between hydrogen atom of the –CH in the ring of PCM and the oxygen atom of –OH in IBP. The calculated intermolecular hydrogen bonding energy (E_{HB}) energies were found as -2.05 and -7.31 kcal/mol for –CH...OH and –OH...C=O interactions, correspondingly. QTAIM calculations propose that the hydrogen bonding interactions mainly and more strongly occur at the –OH...C=O edge. It was also observed that E_{HB} energies altered in different ways that either increased or decreased or stayed constant depending on the site where the hydrogen bondings (HBs) were observed Table 2.

Table 1. Some topological parameters of BCPs for gas phase calculations.

	Type	O...BCP	BCP...H	D	ρ(r)	∇2ρ(r)	H(r)	-G/V	E_{HB}
C1	O44-H45...O33	1.210	0.686	1.896	0.0281	0.0910	-0.0003	0.987	-7.31
	C35-H40...O32	1.543	1.064	2.607	0.0068	0.0246	0.0009	1.205	-2.05
C2	C39-H43...O33	1.431	0.937	2.368	0.0120	0.0378	0.0005	1.059	-2.67
	O32-H16...O44	1.193	0.658	1.851	0.0313	0.0984	-0.0010	0.962	-8.35
C3	O44-H45...O33	1.190	0.654	1.844	0.0350	0.1075	-0.0015	0.950	-9.35
	O32-H16...O44	1.192	0.654	1.846	0.0338	0.1019	-0.0017	0.941	-9.04
C4	O32-H16...O49	1.140	0.597	1.737	0.0411	0.1289	-0.0011	0.968	-10.82
	C50-H53...O33	1.381	0.896	2.277	0.0146	0.0455	0.0003	1.028	-3.39
C5	C6-H30...C38	1.878	1.541	3.419	0.0031	0.0096	0.0019	1.462	-0.41
	C50-H51...O32	1.637	1.148	2.785	0.0056	0.0206	0.0009	1.273	-1.04
	N46-H47...O32	1.330	0.819	2.149	0.0168	0.0550	-0.0002	0.986	-4.39
	C38-H42...O32	1.691	1.211	2.902	0.0043	0.0165	0.0009	1.391	-0.72
C6	C6-H30...C38	1.806	1.308	3.114	0.0037	0.0114	0.0022	1.467	-0.47
	C50-H51...O33	1.574	1.123	2.697	0.0063	0.0230	0.0009	1.231	-1.22
	N46-H47...O33	1.275	0.763	2.038	0.0218	0.0668	-0.0004	0.978	-5.65
	C38-H42...O33	1.679	1.211	2.890	0.0046	0.0179	0.0010	1.400	-0.78

BCP: bond critical point (Å), D: bond length (Å), ρ(r): electron density (a.u.), $\nabla^2\rho(r)$: Laplacian of the electron density, H(r): electron energy density (a.u.), G(r): electron kinetic energy density, V(r): electron potential energy density (a.u.), E_{HB}: hydrogen bonding energy (kcal/mol).

Table 2. Some topological parameters of BCPs for water media calculations.

	Type	O…BCP	BCP…H	D	ρ(r)	$\nabla^2\rho(r)$	H(r)	-G/V	E_{HB}
C1	O44-H45…O33	1.619	0.647	2.266	0.0334	0.1067	-0.0007	0.975	-8.79
	C35-H40…O32	1.544	1.060	2.604	0.0071	0.0252	0.0008	1.174	-1.44
C2	C39-H43…O33	1.481	0.984	2.465	0.0010	0.0321	0.0007	1.104	-2.10
	O32-H16…O44	1.778	0.635	2.413	0.0347	0.1069	-0.0013	0.956	-9.19
C3	O44-H45…O33	1.193	0.656	1.849	0.0346	0.1058	-0.0014	0.952	-9.19
	O32-H16…O44	1.203	0.663	1.866	0.0323	0.0971	-0.0016	0.941	-8.63
C4	O32-H16…O49	1.120	0.571	1.691	0.0467	0.1430	-0.0019	0.952	-12.39
	C50-H53…O33	1.479	0.989	2.468	0.0101	0.0330	0.0006	1.087	-2.16
C5	C38-H42…C6	1.935	1.491	3.426	0.0023	0.0072	0.0014	1.400	-0.31
	C50-H51…O32	1.639	1.147	2.786	0.0054	0.0206	0.0010	1.313	-1.00
	N46-H47…O32	1.309	0.797	2.106	0.0182	0.0593	-0.0002	0.987	-4.77
	C38-H42…O32	1.653	1.166	2.819	0.0050	0.0188	0.0010	1.357	-0.88
C6	C38-H42…C6	1.935	1.491	3.426	0.0021	0.0066	0.0013	1.444	-0.28
	C50-H51…O33	1.579	1.115	2.694	0.0064	0.0236	0.0010	1.256	-1.22
	N46-H47…O33	1.248	0.733	1.981	0.0245	0.0769	-0.0006	0.971	-7.53
	C38-H42…O33	1.619	1.152	2.771	0.0055	0.0205	0.0010	1.313	-1.00

BCP: bond critical point (Å), D: bond length (Å), ρ(r): electron density (a.u.), $\nabla^2\rho(r)$: Laplacian of the electron density, H(r): electron energy density (a.u.), G(r): electron kinetic energy density, V(r): electron potential energy density (a.u.), E_{HB}: hydrogen bonding energy (kcal/mol).

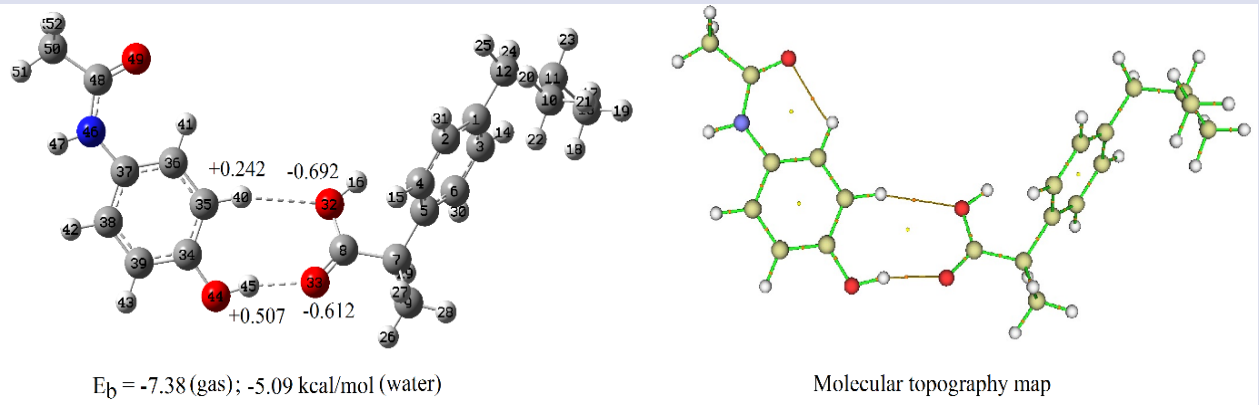

Figure 1. Optimized structure and molecular topography map of C1.

In the interpretation of topological analysis, the electron density ρ(r) and Laplacian of electron density $\nabla^2\rho(r)$ are very important parameters to understand the nature of molecular interactions. Moreover, the ratio of the kinetic electron energy density to the potential electron energy density G(r) / |V(r)| can also be used to analyze the bonding interactions. According to Rozas et. al, if $\nabla^2\rho(r)>0$ and H(r)>0 then HB can be considered as weak. Further, if $\nabla^2\rho(r)>0$ and H(r)<0 then HB interaction is supposed to be medium [29]. Therefore, for C1 conformer at the –CH…OH edge the strength of HB appears as weak, at the –OH…C=O edge it can be regarded as having medium strength. The G(r) / |V(r)| ratio with a value of slightly smaller than 1 (0.987) also refers to a medium type HB interactions for the –OH…C=O edge.

It is also possible to observe the interaction edges by following vibrational frequency shifts at the interacted edges. There are four stretching vibrations at the interaction edges. These are CH&OH of PCM and OH&C=O of IBP. They are shifted around 10, 159, 23 and 31 cm^{-1}, respectively. It is seen that the largest frequency shift appeared at –OH…C=O edge which is previously discussed as having where the medium strength HB interactions occur.

Conformer C2

The optimized structure and the interaction sites for IBP and PCM for C2 are given in Figure 2. NBO charges of C2 at the interaction edges were found as +0.273 / -0.637 for –CH / –C=O and -0.721 / +0.516 for –OH / –OH. E_b energies were calculated as -10.56 and -6.69 kcal/mol correspondingly. In Figure 2, the molecular topography map of the system can also be seen. For C2, two possible intermolecular HBs were taken into account. The first one is between the hydrogen of the –CH in the ring of PCM and the oxygen of –C=O in IBP. The second one is between –OHs of PCM and IBP. E_{HB} energies were found as -2.67 and -8.35 kcal/mol for –CH…–C=O and –OH…–OH interactions, respectively. According to QTAIM findings, HB interactions more strongly occur at the –OH…–OH edge. For –CH…–C=O interactions $\nabla^2\rho(r)$ and H(r) were found as positive. Thus, HB can be considered as weak at this edge. As for the –OH…–OH edge while $\nabla^2\rho(r)$ were found as positive, H(r) appeared as negative. Henceforth, HB interaction is supposed to be medium. The G(r) / |V(r)| ratio for the related edges also suggest that medium type HB interactions for the –OH…–OH edge (0.962) and a weak type of HB for –CH…–C=O edge (1.059).

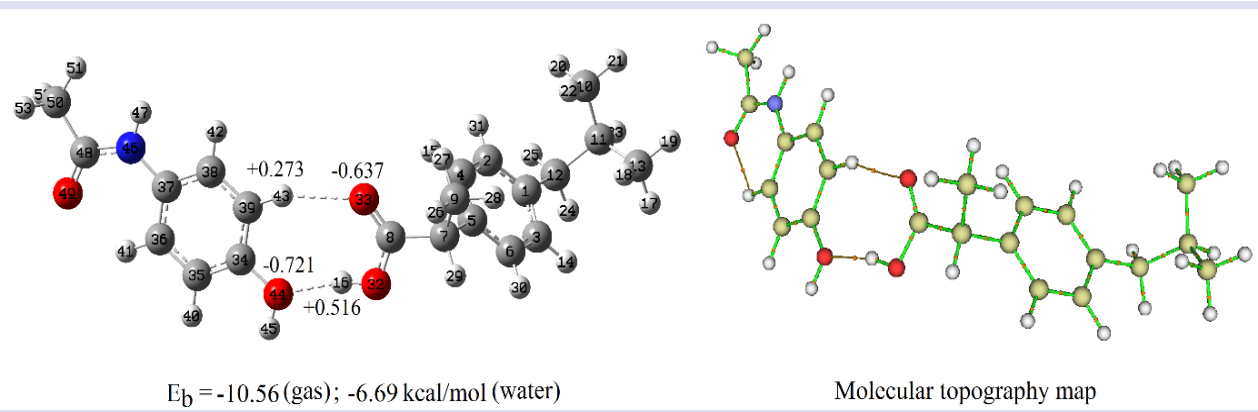

Figure 2. Optimized structure and molecular topography map of C2

In the C2 again, there are four stretching vibrations at the interaction sites. These are CH&OH of PCM and C=O&OH of IBP. They are shifted around 12, 8, 63 and 192 cm^{-1} correspondingly. The largest frequency shift was observed at –OH…–OH edge which confirms where the medium strength HB interactions occur.

Conformer C3

The optimized structure for C3 is given in Figure 3. NBO charges of C3 at the interaction sites were found as +0.512 / -0.659 for –OH / –C=O and -0.744 / +0.516 for –OH / –OH. E_b energies were calculated as -13.60 and -7.59 kcal/mol, respectively. In Figure 3, the molecular topography map of the system is given. Two possible HBs were suggested between OH of PCM and OH&C=O of IBP. E_{HB} energies were found as -9.35 and -9.04 kcal/mol for –OH…–C=O and –OH…–OH interactions respectively. QTAIM findings propose that HB interactions almost occur at the same strength for both interaction sites. Both interaction sites yielded positive $\nabla^2\rho(r)$ and negative H(r) values. Thus, HB interactions can be considered as medium strength. The G(r) / |V(r)| ratios were found slightly smaller than 1 for both edges also indicating the medium type of HB interactions.

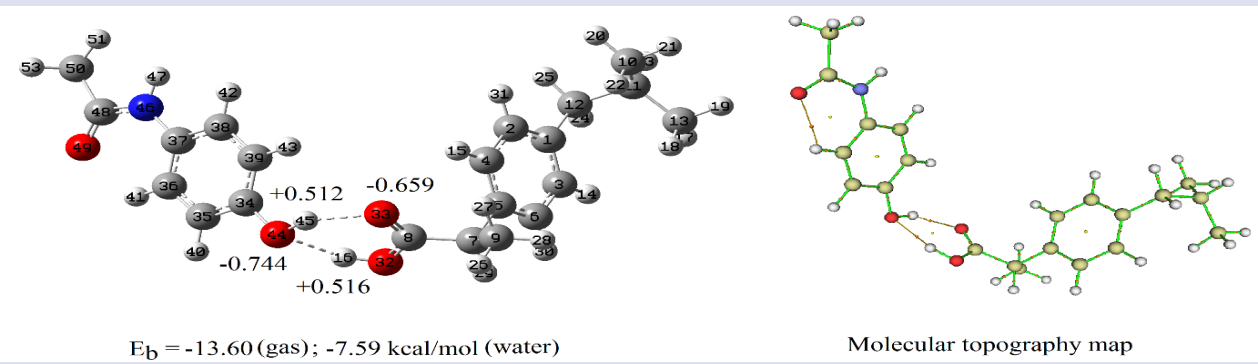

Figure 3. Optimized structure and molecular topography map of C3.

In the C3 conformer, taking the oxygen atom of PCM at the center, symmetric and antisymmetric vibrations were observed (Figure 4). The frequency shifts for OH of PCM were observed as 285 and 377 cm^{-1} for symmetric and antisymmetric vibrations correspondingly. C=O stretching vibrations of PCM was also shifted around 95 cm^{-1} upon interaction. Further, the frequency shifts for OH of IBP were calculated as 214 and 306 cm^{-1}, respectively.

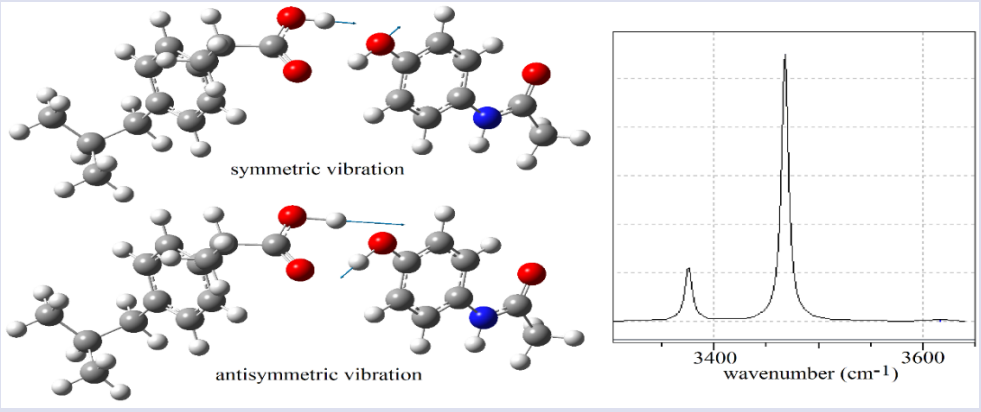

Figure 4. Symmetric and antisymmetric vibrational behavior of hydroxyl groups and their vibrational spectroscopic infrared bands.

Conformer C4

The optimized structure of C4 is given in Figure 5. NBO charges of C4 at the interaction edges were found as -0.670 / +0.517 for –C=O / –OH and +0.293 / -0.650 for –CH_3 / –C=O. The obtained E_b energies (gas/water) were found as -13.75 and -9.23 kcal/mol, respectively. In Figure 5, the molecular topography map of the system is also given. For this configuration, two possible intermolecular HBs seem possible. The first one is between the oxygen of the carbonyl group in PCM and the hydrogen of the hydroxyl group in IBP. The second possibility is between one of the hydrogens in the methyl group of PCM and the oxygen of the carbonyl group in IBP. E_{HB} energies were found as -10.82 and -3.39 kcal/mol for –C=O…-OH and –CH_3…–C=O interactions, respectively. It is clearly seen that HB interaction occurs primarily at the –C=O…–OH site where the $\nabla^2\rho(r)$ is positive and H(r) is negative addressing a medium type of interaction. At the same site the G(r) / |V(r)| ratio was found as 0.968 which confirms the previous assumption for the medium type HB connections. With both positive $\nabla^2\rho(r)$ and H(r) values and a G(r) / |V(r)| ratio larger than 1 the –CH_3…–C=O edge shows weak HB interactions. The largest vibrational shift with a value of 405 cm^{-1} in the infrared spectrum was observed with –OH of IBP which indicates that the strongest HB interactions occurs at –C=O…–OH site.

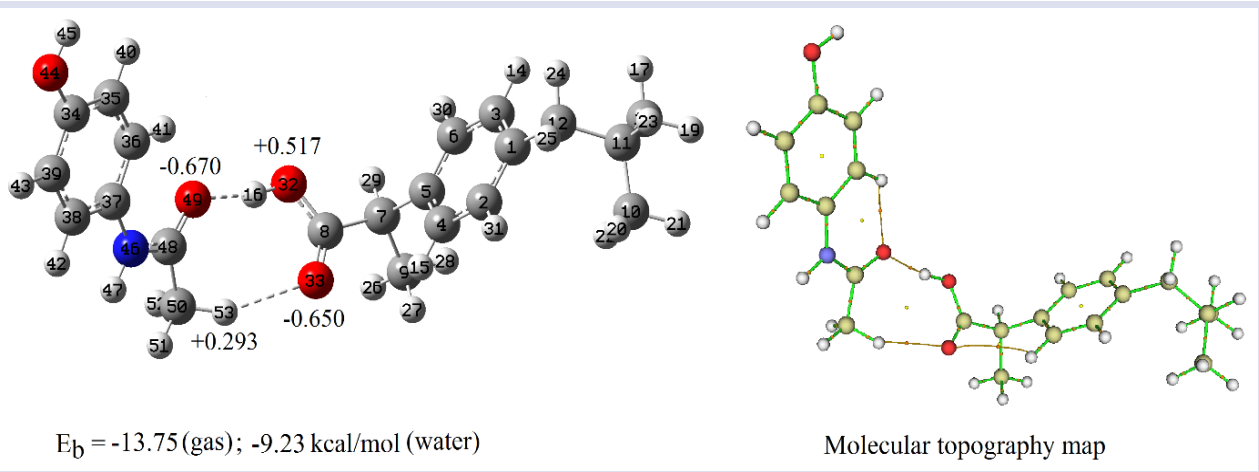

Figure 5. Optimized structure and molecular topography map of C4.

Conformer C5

The optimized structure for C5 is presented in Figure 6. NBO charges of C5 at the interaction edges were observed as -0.739 / +0.430 for –OH / –NH with E_b energies of -6.73 and -3.37 kcal/mol for gas phase and water media calculations, respectively. For C5, four intermolecular HBs were suggested by the topography map (Figure 6). However, if Table 1 is examined, it is seen that three of them is very weak in strength. The strongest HB based on the E_{HB} evaluations was identified between –NH of PCM and –OH of IBP. E_{HB} energy for this site was found as –4.39 kcal/mol with positive $\nabla^2\rho(r)$ and slightly negative H(r) (-0.0002) and with slightly smaller than 1 (0.986) G(r) / |V(r)| ratio indicating that the HB interaction is somewhere between medium and weak. The largest vibrational frequency shift in the infrared spectrum was observed with –NH of PCM with a value of 46 cm^{-1}.

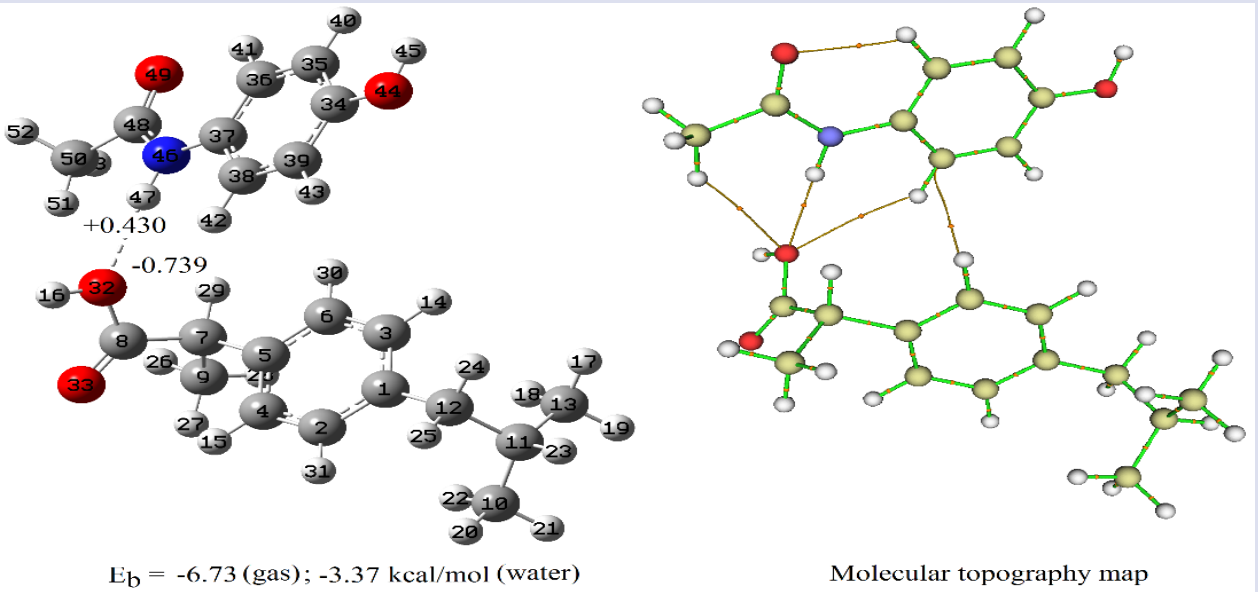

Figure 6. Optimized structure and molecular topography map of C5.

Conformer C6

NBO charges of C6 at the interaction edges were found as -0.638 / +0.438 for –C=O / –NH as can be seen in Figure 7. For gas and water media, E_b energies were found at -8.00 and -3.93 kcal/mol, respectively. C6 shows again four possible intermolecular HB interactions (Figure 7) but only HB between –C=O of IBP and –NH of PCM with E_{HB} energy of -5.65 kcal/mol seems strong (Table 1). In this interaction site $\nabla^2\rho(r)$ was found as positive and H(r) appeared as negative with a G(r) / |V(r)| ratio slightly smaller than one (0.978) indicating nearly a medium type of HB interaction. The largest vibrational frequency shift in the infrared spectrum of C6 was observed with –NH of PCM with a value of 165 cm^{-1}.

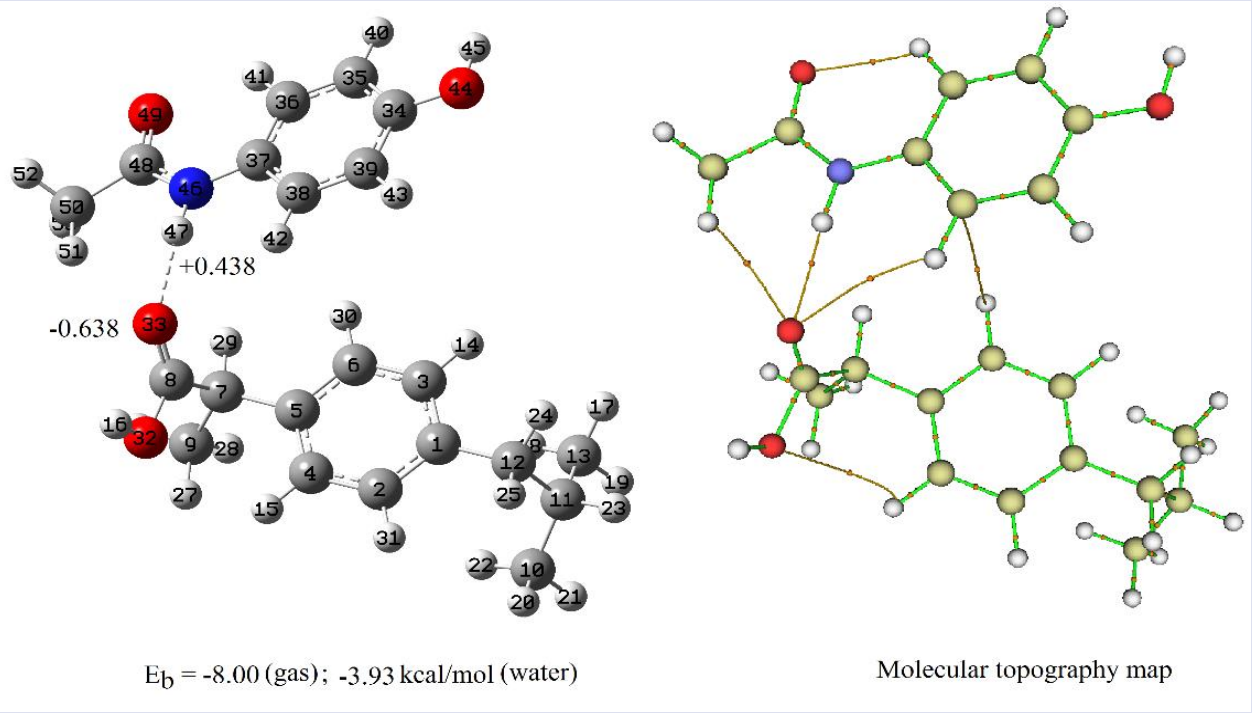

Figure 7. Optimized structure and molecular topography map of C6.

Structure–Activity Relationship

DFT was also used to search the relationships between biological activity and structure which are based on the fundamental hypothesis that biological properties are functions of the molecular structure [11, 30]. As an example, the antibacterial activity is related to the function of the lowest unoccupied molecular orbital (LUMO). Compounds which have low LUMO energy are more highly motivated to accept electrons than those with higher energy since incoming electrons are received in LUMO. LUMO energies of C1-C6 conformers were found as -0.786 (-0.484), -0.152 (-0.299), -0.434 (-0.472), -0.395 (-0.451), -0.607 (-0.481) and -0.731 (-0.570) eV correspondingly (water) while the energies of LUMO for IBP and PCM were observed as -0.563 (-0.350) and -0.074 (-0.200). C1 has the lowest LUMO energy in the gas phase whereas C6 has the lowest value in water. In addition, C1 and C6 have also lower LUMO energies in gas and water medium as compared to all the other conformers studied in this work. Thus, one can conclude the C1 or C6 conformers show higher biological activities.

Band gap (E_g) energies between the highest occupied and lowest unoccupied molecular orbitals (HOMO-LUMO) of C1-C6 conformers were found as 4.045 (4.947), 5.507 (5.458), 5.088 (5.223), 5.348 (5.303), 4.741 (5.065) and 4.446 (4.933) eV correspondingly (water) while the energies of LUMO for IBP and PCM were observed as 6.118 (6.213) and 5.403 (5.402). The values of the lowest E_g of C1-C6 conformers show same trends with the LUMO energies.

Physicochemical properties and druglikeness

The physicochemical properties give a global description of the structures of compounds. Bioavailability radar of the compounds displays a rapid evaluation of druglikeness. As seen in Table 3 and Figure 8, the bioavailability radar includes six physicochemical properties [28, 31]. In Figure 8, the pink area represents the optimal range of these properties and the red line represents the properties of the compounds. The red lines of IBP…PCM system are in the range of the pink area. Therefore, we can conclude that the interacted compounds are orally predicted bioavailable. Furthermore, druglikeness was established based on the physicochemical properties to find oral drug candidates [28]. There are five different rule-based filters which are defined as follows: (1) Lipinski's filter includes molecular weight ≤ 500, MLOGP (lipophilicity) ≤ 4.15, hydrogen bond acceptors ≤ 10, and hydrogen bond donors ≤ 5 [32]. (2) Ghose's filter includes 160 ≤ molecular weight ≤ 480, −0.4

≤ WLOGP (lipophilicity) ≤ 5.6, 40 ≤ the molar refractivity ≤ 130, and 20 ≤ number of atoms ≤ 70 [33]. (3) Veber's filter includes the number of rotatable bonds ≤ 10 and the total polar surface area ≤ 140 [34]. (4) Egan's filter includes WLOGP (Lipophilicity) ≤ 5.88 and the total polar surface area ≤ 131.6 [35]. (5) Muegge's filter includes 200 ≤ molecular weight ≤ 600, −2 ≤ XLOGP3 (lipophilicity) ≤ 5, the total polar surface area ≤ 150, the number of rings ≤ 7, the number of carbon > 4, the number of heteroatoms > 1, the number of rotatable bonds ≤15, the hydrogen bond acceptors ≤10, and the hydrogen bond donors ≤ 5 [36]. The result of drug-likeness evaluation of IBP…PCM is also shown in Figure 8 and we can conclude that IBP…PCM system fulfil all requirements of Lipinski, Ghose, Veber, Egan and Muegge rules.

Table 3. Physicochemical properties, lipophilicity and solubility of IBP…PCM.

Properties	Bioavailability	IBP…PCM
Molecular weight	Size (between 150 and 500 g/mol)	357.44
Heavy atom		26
Arom. heavy atom		12
Fraction Csp3	Saturation (not less than 0.25)	0.33
Rotatable Bond	Flexibility (not more than 9)	6
H-Bond acceptor		4
H-Bond donor		3
Molar refractivity		104.96
Polar surface area	Polarity (between 20 and 130 Å^2)	86.63
Lipophilicity		
MLOGP		3.12
WLOGP		4.23
XLOGP3	Lipophilicity (between -0.7 and +5.0)	4.24
Water Solubility	Solubility (log S not higher than 6)	
ESOL		-4.67
ALI		-5.77
SILICOS-IT		-3.44

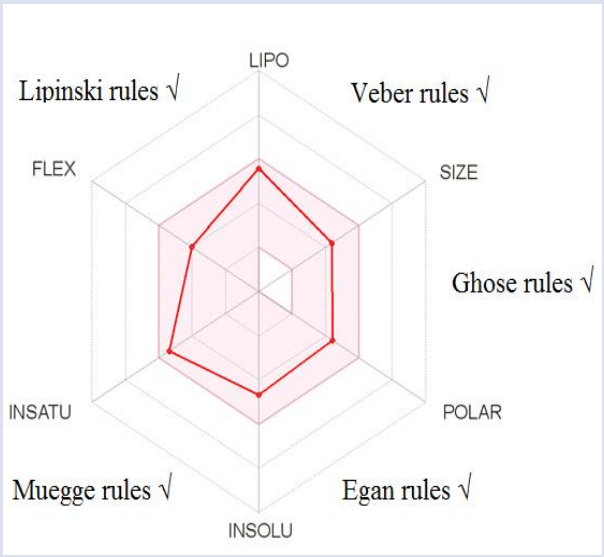

Figure 8. Bioavailability radar of IBP…PCM.

Conclusions

A detailed DFT, NBO charge and QTAIM investigations of PCM interacted IBP were carried out. The stabilities based on the binding energies of the PCM&IBP system decreased in water media calculations. C4 appeared as the most stable conformer based on the results of E_b and E_{HB} calculations in both environments. Further, all of the results obtained indicate that the strength of the interactions occurs at the physisorption level. In general, it was observed that as the interaction strength increases the larger vibrational frequency shifts were observed in the vibrational frequencies of molecular fragments at the interaction sites. The findings of this work are supposed to enlighten further biological activity studies of PCM and IBP combinations. Among the six configurations, C1 and C6 showed better biological activity. The field is further open for pharmacokinetics and clinic studies. It is also worth to note that combinations of IBP and PCM showed lower LUMO values indicating that the activity of combinations of these drugs is higher when they are used together. The drug-likeness study revealed that the interacted compounds (IBP…PCM) fulfill all requirements of Lipinski, Ghose, Veber, Egan, and Muegge rules and IBP…PCM is predicted orally bioavailable. These preliminary results provide the lead for the design of more potent and selective covid drugs.

Acknowledgment

This work was supported by Eskişehir Technical University (Project Number 20ADP133).

Conflicts of interest

There are no conflicts of interest in this work.

References

[1] Roushani M., Shahdost-Fard F., Applicability of AuNPs@N-GQDs nanocomposite in the modeling of the amplified electrochemical Ibuprofen aptasensing assay by monitoring of riboflavin, *Bioelectrochemistry*, 126 (2019) 38-47.

[2] Lazarević J.J., Uskoković–Marković S., Jelikić–Stankov M., Radonjić M., Tanasković D., Lazarević N., Popović Z.V., Intermolecular and low-frequency intramolecular Raman scattering study of racemic ibuprofen, *Spectrochim. Acta A.*, 126 (2014) 301-305.

[3] Fanali G., di Masi A., Trezza V., Marino M., Fasano M., Ascenzi P., Human serum albumin: From bench to bedside, *Mol Aspects Med.,* 33(3) (2012) 209-290.

[4] Anderson B.J., Paracetamol (acetaminophen): mechanisms of action, *Paediatr Anaesth.*, 18(10) (2008) 915-921.

[5] Langhendries J.P., Allegaert K., Van Den Anker J.N., Veyckemans F., Smets F., Possible effects of repeated exposure to ibuprofen and acetaminophen on the intestinal immune response in young infants, *Med. Hypotheses*, 87 (2016) 90-96.

[6] Derry C.J., Derry S., Moore R.A., Single dose oral ibuprofen plus paracetamol (acetaminophen) for acute postoperative pain, *Cochrane Database Syst. Rev.,* (6) CD010210 (2013).

[7] Doherty M., Hawkey C., Goulder M., Gibb I., Hill N., Aspley S., Reader S., A randomised controlled trial of ibuprofen, paracetamol or a combination tablet of ibuprofen/paracetamol in community-derived people with knee pain, *Ann. Rheum. Dis.*, 70(9) (2011) 1534-1541.

[8] Eccles R., Holbrook A., Jawad M., A double-blind, randomised, crossover study of two doses of a single-tablet combination of ibuprofen/paracetamol and placebo for primary dysmenorrhoea, *Curr. Med. Res. Opin.,* 26 (11) (2010) 2689-2699.

[9] Mehlisch D.R., Aspley S., Daniels S.E., Bandy D. P., Comparison of the analgesic efficacy of concurrent ibuprofen and paracetamol with ibuprofen or paracetamol alone in the management of moderate to severe acute postoperative dental pain in adolescents and adults: a randomized, double-blind, placebo-controlled, parallel-group, single-dose, two-center, modified factorial study, *Clin. Ther.,* 32(5) (2010) 882-895.

[10] Merry A.F., Gibbs R.D., Edwards J., Ting G.S., Frampton C., Davies E., Anderson B.J., Combined acetaminophen and ibuprofen for pain relief after oral surgery in adults: a randomized controlled trial, *Br. J. Anaesth.*, 104(1) (2010) 80-88.

[11] Kawakami J., Kakinami H., Matsushima N., Nakane A., Kitahara H., Nagaki M., Ito S., Structure-activity relationship analysis for antimicrobial activities of tryptanthrin derivatives using quantum chemical calculations, *J. Comput. Chem. Jpn.,* 12(2) (2013) 109-112.

[12] Venkataramanan N.S., Suvitha A., Kawazoe Y., Intermolecular interaction in nucleobases and dimethylsulfoxide/water molecules: A DFT, NBO, AIM and NCI analysis, *J. Mol. Graph. Model.*, 78 (2017) 48–60.

[13] Ravaei I., Haghighat M., Azami S.M., A DFT, AIM and NBO study of isoniazid drug delivery by MgO nanocage, *Appl. Surf. Sci.,* 469 (2019) 103–112.

[14] Lu T., Chen F., Multiwfn: a multifunctional wavefunction analyzer, *J. Comput. Chem.*, 33 (2012) 580–592.

[15] Bader R.F.W., Atoms in Molecules: A Quantum Theory, Clarendon, New York, 1990.

[16] Reed A.E., Weinstock R.B., Weinhold F., Natural population analysis, *J. Chem. Phys.*, 83 (1985) 735–746.

[17] Reed A.E., Curtiss L.A., Weinhold F., Intermolecular interactions from a natural bond orbital, donor-acceptor viewpoint, *Chem. Rev.*, 88 (1988) 899–926.

[18] Alver Ö., FT-IR, Raman and DFT Studies on the vibrational spectra of 2,2-bis(aminoethoxy)propane, *Bull. Chem. Soc. Ethiop.*, 30(1) (2016) 147-151.

[19] Hadad A., Azevedo D.L., Caetano E.W.S., Freire V.N., Mendonça G.L.F., Neto P.L., Albuquerque E.L., Margis R., Gottfried C., Two-level adsorption of ibuprofen on C60 fullerene for transdermal delivery: classical molecular dynamics and density functional theory computations, *J. Phys. Chem. C.*, 115(50) (2011) 24501-24511.

[20] Saikia U., Saikia N., Waters K., Pandey R., Sahariah M.B., Electronic properties of acetaminophen adsorbed on 2D clusters: A first principles density functional study, *Chemistry Select.,* 2(13) (2017) 3613-3621.

[21] Dennington R.D., Keith T.A., Millam J.M., GaussView 5.0.8, Gaussian Inc., 2008.

[22] Parlak C., Alver Ö., A density functional theory investigation on amantadine drug interaction with pristine and B, Al, Si, Ga, Ge doped C60 fullerenes, *Chem. Phys. Lett.*, 678 (2017) 85-90.

[23] Boys S.F., Bernardi F., The calculation of small molecular interactions by the differences of separate total energies. Some procedures with reduced errors, *Mol. Phys.*, 19(4) (1970) 553-566.

[24] Gutowski M., Chalasinski G., Critical evaluation of some computational approaches to the problem of basis set superposition error, *J. Chem. Phys.,* 98 (1993) 5540-5554.

[25] Beheshtian J., Peyghan A.A., Bagheri Z., Carbon nanotube functionalization with carboxylic derivatives: a DFT study, *J. Mol. Model.,* 19(1) (2013) 391–396.

[26] Peyghan A.A., Soltani A., Pahlevani A.A., Kanani Y., Khajeh S., A first-principles study of the adsorption behavior of CO on Al- and Ga-doped single-walled BN nanotubes, *Appl. Surf. Sci.*, 270 (2013) 25–32.

[27] Frisch M.J., Trucks G.W., Schlegel H.B., Gaussian 09, Revision A.1, Gaussian Inc., Wallingford, CT, 2009.

[28] Daina A., Michielin O., Zoete V., SwissADME: a free web tool to evaluate pharmacokinetics, drug-likeness and medicinal chemistry friendliness of small molecules. *Sci Rep.,* 42717(7) (2017).

[29] Rozas I., Alkorta I., Elguero J., Behavior of ylides containing N, O and C atoms as hydrogen bond acceptors, *J. Am. Chem. Soc.,* 122(45) (2000) 11154-11161.

[30] Bhattacharjee A.K., Skanchy D.J., Jennings B., Hudson T.H., Brendle J.J., Werbovetz K.A., Analysis of stereoelectronic properties, mechanism of action and pharmacophore of synthetic indolo[2,1-b]quinazoline-6,12-dione derivatives in relation to antileishmanial activity using quantum chemical, cyclic voltammetry and 3-D-QSAR Catalyst procedures, *Bioorg. Med. Chem.,* 10 (6) (2002) 1979-1989.

[31] Al Wasidi A.S., Hassan A.S., Naglah A.M., In vitro cytotoxicity and druglikeness of pyrazolines and pyridines bearing benzofuran moiety, *J. Appl. Pharm. Sci.*, 10(4) (2020) 142–148.

[32] Lipinski C.A., Lombardo F., Dominy B.W., Feeney P.J., Experimental and computational approaches to estimate solubility in drug discovery and development settings, *Adv. Drug. Deliv. Rev.,* 46(1-3) (2001) 3-26

[33] Ghose A.K., Viswanadhan V.N., Wendoloski J.J., A knowledge-based approach in designing combinatorial or medicinal chemistry libraries for drug discovery. 1. A qualitative and quantitative characterization of known drug databases, *J. Comb. Chem.,* 1(1) (1999) 55-68.

[34] Veber D.F., Johnson S.R., Cheng H.-Y., Smith B.R., Ward K.W., Kopple K.D., Molecular properties that influence the oral bioavailability of drug candidates, *J. Med. Chem.,* 45(12) (2002) 2615-2623.

[35] Egan W.J., Merz K.M., Baldwin J.J., Prediction of drug absorption using multivariate statistics, *J. Med. Chem.*, 43(21) (2000) 3867-3877.

[36] Muegge I., Heald S.L., Brittelli D., Simple selection criteria for drug-like chemical matter, *J. Med. Chem.,* 44(12) (2001) 1841-1846.